Volume 17 | Number 24 | 28 June 2015 | Pages 4411–4602

CrystEngComm

www.rsc.org/crystengcomm

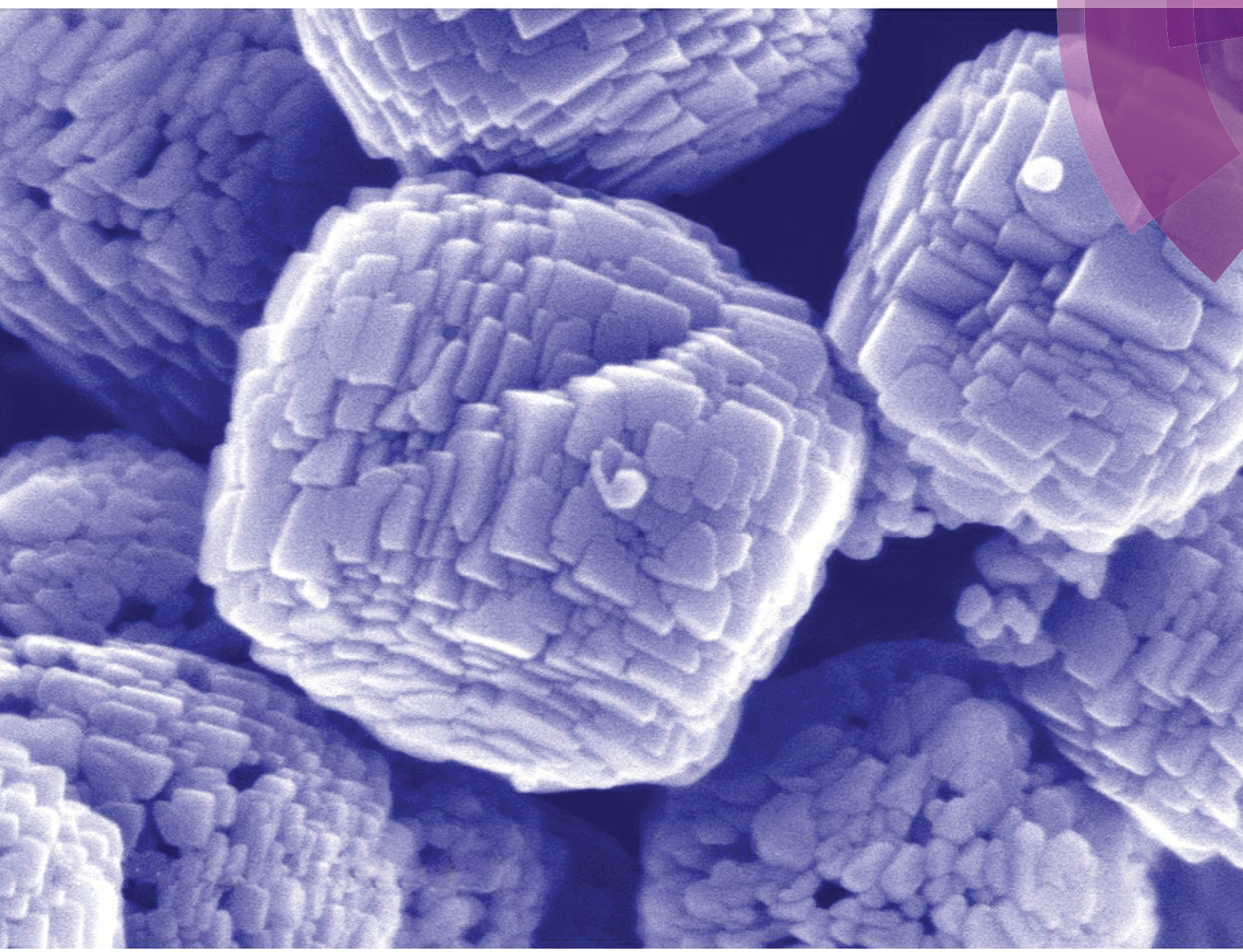

ROYAL SOCIETY OF CHEMISTRY

PAPER

Rongmei Liu *et al.*

Cu^{2+} ions inducing the growth of porous Co_3O_4 nanospheres as high-capacity supercapacitors

CrystEngComm

PAPER

View Article Online
View Journal | View Issue

Cite this: *CrystEngComm*, 2015, **17**, 4449

Cu^{2+} ions inducing the growth of porous Co_3O_4 nanospheres as high-capacity supercapacitors

Rongmei Liu,*[a] Zixiang Jiang,[a] Qi Liu,[b] Xiandong Zhu[a] and Weiye Chen[a]

Received 3rd April 2015,
Accepted 10th May 2015

DOI: 10.1039/c5ce00658a

www.rsc.org/crystengcomm

Published on 11 May 2015. Downloaded on 9/25/2024 5:25:34 AM.

In this study, porous Co_3O_4 nanospheres were controllably synthesized by applying metal Cu^{2+} ions as structure-inducing agents. The growth of the Co_3O_4 nanostructures was induced by the metal ions without the addition of any surfactants. The porous Co_3O_4 nanospheres were composed of nanosheets. When used as electrode materials in a supercapacitor, the porous Co_3O_4 nanospheres exhibited a much better capacity of 246.7 F g^{-1} than commercial Co_3O_4 powder at a current density of 0.5 A g^{-1}, maintaining 86% of the initial capacity at a current density of 1 A g^{-1} after 500 cycles. Such high performance can be attributed to the desirable morphology. The results manifest that porous Co_3O_4 nanospheres composed of nanosheets are promising electrode materials for supercapacitors.

Introduction

Cobalt oxide, as an important transition metal oxide, has been widely studied and used in many fields such as gas sensors,[1–4] heterogeneous catalysis,[5,6] lithium-ion batteries,[7,8] supercapacitors[9–11] and magnetic materials[12] due to its conspicuous physico-chemical properties and low cost. As an electrode material for supercapacitors, cobalt oxide has been thought to be one of the most promising electrode materials for next-generation high-performance supercapacitors due to its high theoretical specific capacitance, good electrochemical reversibility, and low cost.[13] Nanosized cobalt oxide has attracted great interest due to the significant nano-effects different from those of bulk materials. Diverse shapes and morphologies of cobalt oxide nanomaterials such as wires,[14] rods,[15] tubes,[16] polyhedra,[17] sheets,[6] flowers[18] and spheres[19] were successfully synthesized. Among these shapes, nanomaterials with porous or hollow structures have received much attention because of their high surface area, fast ion transfer and many exposed centers, which show great application potential in batteries, absorbents, catalysts, *etc.* Up to now, many methods have been used to fabricate hollow Co_3O_4 structures such as the complex precursor-calcination method,[20,21] template-based chemical vapor deposition,[22] solvothermal treatment,[23] micro-emulsion method[24] and so on. Among these methods, the complex precursor-calcination method is the most used method. For example, Du *et al.* first prepared one-dimensional cobalt acetate hydroxide ($Co_5(OH)_2(CH_3COO)_8{\cdot}2H_2O$) prisms as the precursor, and then through thermal decomposition synthesized hollow Co_3O_4 nanoboxes.[20] Shi *et al.* obtained one-dimensional Co_3O_4 nanotubes by thermal decomposition of a Co(III) complex with strong intermolecular hydrogen bonding precursors.[16]

Metal ions have been demonstrated to control the shape and morphology of nanomaterials.[25] We have used different metal ions as structure-inducing agents to synthesize differently-shaped α-Fe_2O_3 nanocrystals.[26] In this paper, we provided a new method for the controllable synthesis of porous and hollow Co_3O_4 nanospheres by using metal Cu^{2+} ions as structure-inducing agents and ammonium solution as the alkali source through hydrothermal reaction. The porous Co_3O_4 nanospheres were composed of nanosheets. In the electrochemical measurements, the porous Co_3O_4 nanospheres exhibited a much better capacity of 246.7 F g^{-1} than commercial Co_3O_4 powder at a current density of 0.5 A g^{-1}, maintaining 86% of the initial capacity at a current density of 1 A g^{-1} after 500 cycles. Such high performance can be attributed to the desirable exposed facet and morphology. The results manifest that porous Co_3O_4 nanospheres composed of nanosheets are promising electrode materials for supercapacitors.

Experimental section

Preparation of porous Co_3O_4 nanospheres

In a typical procedure, the starting solution was prepared by mixing 0.199 g of copper acetate (analytically pure) in 10 mL of 0.2 M $CoSO_4$ solution under magnetic stirring. Then 1 mL of ammonia solution (25%, analytically pure) was added. After 10 min of stirring, the mixture was transferred to and sealed in a 50 mL Teflon-lined autoclave, kept at 160 °C for

[a] *College of Biological and Chemical Engineering, Anhui Polytechnic University, Wuhu, Anhui 241000, PR China. E-mail: liurongmei@ahpu.edu.cn; Fax: +86 553 2871 255; Tel: +86 553 2871 255*
[b] *College of Materials Science and Engineering, Anhui Polytechnic University, Wuhu, Anhui 241000, PR China*

Published on 11 May 2015. Downloaded on 9/25/2024 5:25:34 AM.

12 h, and finally cooled to room temperature. The precipitate was collected by centrifugation (10 000 rpm, 1 min), washed alternately with deionized water and ethanol, and dried in air under ambient conditions.

Characterization

Scanning electron microscopy (SEM) characterization was performed on a Hitachi S-4800 at 5 kV. Transmission electron microscopy (TEM) images were obtained using a JEOL JEM-2100 transmission electron microscope operating at 200 kV. Powder X-ray diffraction (XRD) patterns were collected using a Bruker D8 ADVANCE diffractometer with Cu K_α radiation (λ = 1.5418 Å). X-ray photoelectron spectra (XPS) were collected using an ESCALab MKII X-ray photoelectron spectrometer with non-monochromatized Al Kα X-ray as the excitation source. The binding energies were corrected for specimen charging by calibrating the C1s peak to 284.6 eV.

Electrochemical measurements

In the electrochemical experiments, we used the traditional three-electrode system. The working electrode was prepared by mixing 80 wt% electroactive material (Co_3O_4), 15 wt% acetylene black, and 5 wt% polytetrafluoroethylene. This mixture was then pressed onto the foamed nickel electrode and dried at 60 °C for 12 h. The electrolyte used was 1 M KOH aqueous solution. The capacitive performance of the samples was evaluated on a CHI 660e electrochemical workstation. Cyclic voltammetry and chronopotentiometry were performed in a three-electrode cell where Pt wire served as the counter electrode and a standard calomel electrode (SCE) as the reference electrode.

Results and discussion

The porous nanospheres were prepared by hydrothermally treating a mixture of $CoSO_4$ and ammonium solution with the metal salt $CuAc_2$. Fig. 1 presents the XRD pattern of the as-prepared sample controlled by Cu^{2+}. Almost all of the diffraction peaks can be indexed to the cubic phase of Co_3O_4 (JCPDS 73-1701), indicating that relatively pure Co_3O_4 products were obtained under synthetic conditions. Since the synthesis system has Cu, XPS measurements were also used to identify the Cu content. Fig. 2a demonstrates the presence of Co, Cu and O. The high resolution XPS spectrum in Fig. 2b shows the binding energies of $Cu2p_{3/2}$ and $Cu2p_{1/2}$ corresponding to 933 eV and 953 eV with weak intensities. Fig. 2c shows the binding energies of $Co2p_{3/2}$ and $Co2p_{1/2}$

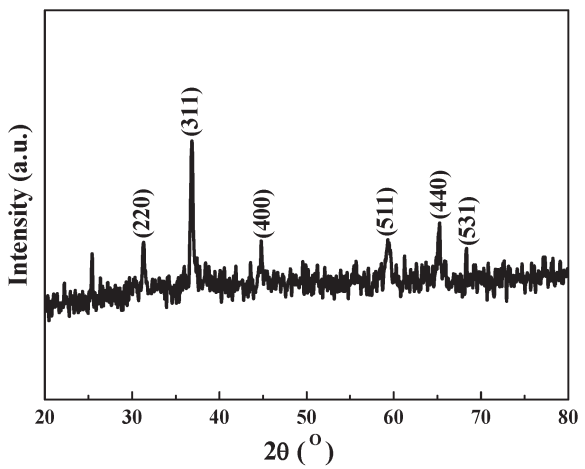

Fig. 1 XRD pattern of the obtained sample.

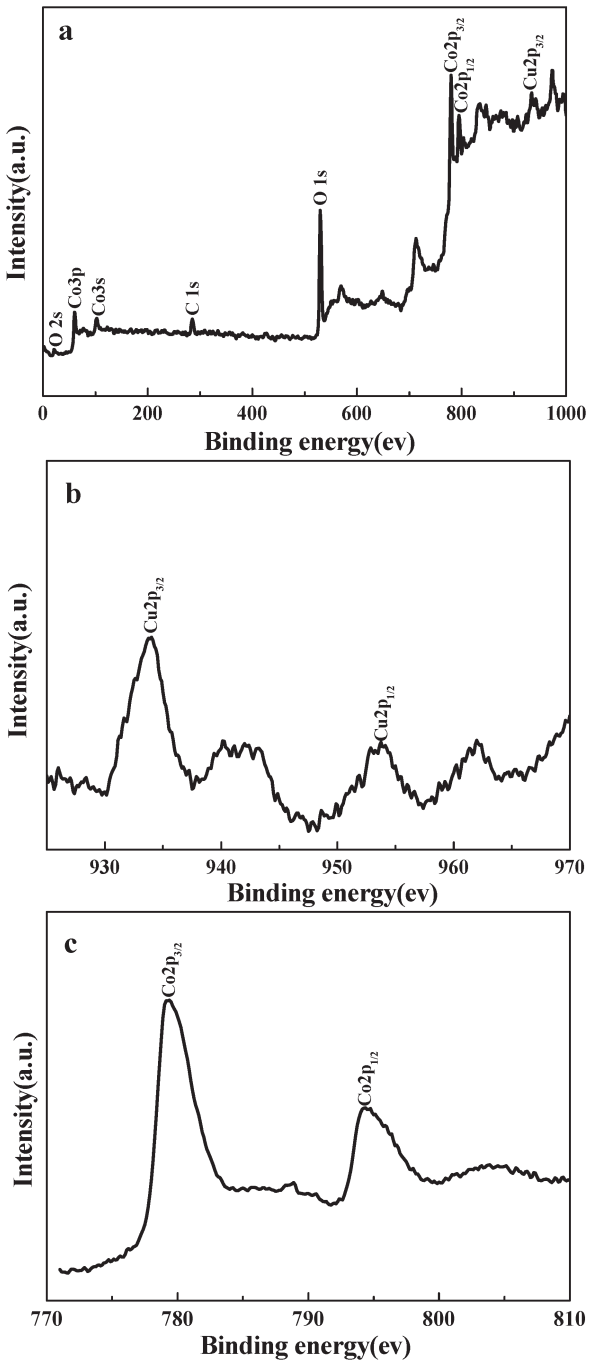

Fig. 2 (a) XPS spectrum, (b) Cu 2p spectrum, and (c) Co 2p spectrum of the obtained sample.

This journal is © The Royal Society of Chemistry 2015

Published on 11 May 2015. Downloaded on 9/25/2024 5:25:34 AM.

corresponding to 778 eV and 793 eV with strong intensities. The Cu/Co atomic ratio obtained by XPS is very small and the XPS results indicate that the Co_3O_4 product controlled by Cu^{2+} is relatively pure Co_3O_4.

Fig. 3a shows a representative large area SEM image of the obtained Co_3O_4, displaying that the majority of the sample is monodisperse spherical nanocrystals with an average diameter of about 400 nm. From the high-magnification SEM images shown in Fig. 3b and c, it can be seen that these nanospheres are composed of nanosheets with a thickness of several nanometers. Fig. 3d–f show the TEM images and HRTEM image of the sample, verifying that the obtained sample is monodisperse, spherical and porous. Fig. 3f also confirms that these nanospheres are composed of nanosheets with a thickness of several nanometers. The HRTEM image shown in Fig. 3f inset displays one type of facet with a crystal plane spacing of about 2.43 Å, corresponding to the (311) facet of the cubic phase of Co_3O_4.

The addition of $CuAc_2$ in the reaction system is undoubtedly the major reason for the formation of Co_3O_4 nanospheres. Without the addition of $CuAc_2$, when the mixture of $CoSO_4$ and ammonium solution was hydrothermally treated, as shown in Fig. 4, only Co_3O_4 microflowers with a much larger size (5 μm) and irregular Co_3O_4 nanoparticles were obtained. With the addition of Cu^{2+}, $CuCo_2O_4$ tends to form under alkali conditions. However, Cu^{2+} can react easily with $NH_3{\cdot}H_2O$ to form a $[Cu(NH_3)_4]^{2+}$ complex and dissolve into the solution, so under the synthetic conditions with $NH_3{\cdot}H_2O$, we can only get Co_3O_4 as the product. In the reaction system, metal ions act as the structure and surface directors. They would be adsorbed on the Co_3O_4 surface and induce the Co_3O_4 nanoparticles to grow into nanocrystals. In order

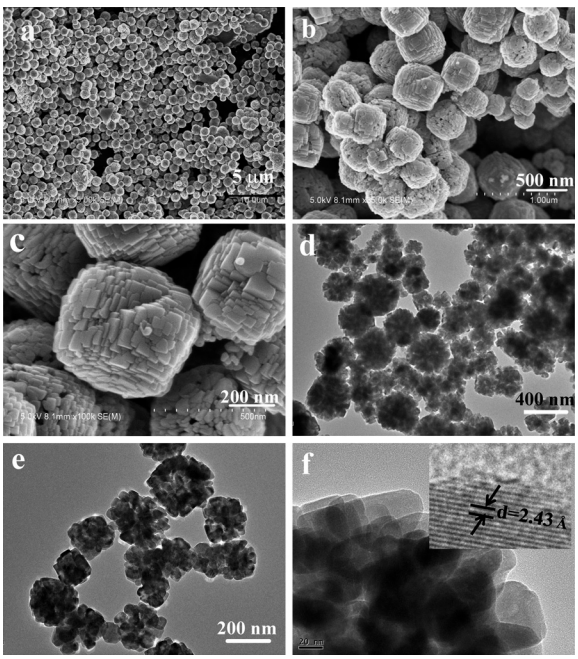

Fig. 3 (a–c) SEM images and (d–f) TEM images (inset in f: HRTEM image) of the porous Co_3O_4 nanospheres.

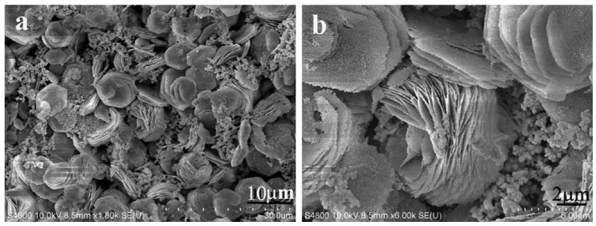

Fig. 4 (a, b) SEM images of the sample synthesized without Cu^{2+} ions.

to prove our assumption that the metal ions are the structure and surface directors rather than Ac^-, $CuCl_2$ and $CuSO_4$ were used respectively as additives to replace $CuAc_2$. As shown in Fig. 5, all the obtained products are Co_3O_4 nanocrystals with a spherical morphology, confirming that the existence of Cu^{2+} is the main reason for the growth of Co_3O_4 nanocrystals.

In order to further confirm that Cu^{2+} is the main reason for the growth of Co_3O_4 nanocrystals, we added the metal salts $CoSO_4$ to the mixture of $CuAc_2$ and ammonium solution and treated the mixture under hydrothermal conditions. The results are shown in Fig. 6. Fig. 6a–c show the SEM images of the obtained product, displaying that the majority of the sample is also monodisperse spherical nanocrystals with an average diameter of about 400 nm, which is almost the same as the typical sample with a different reaction order. Fig. 6d gives the XRD pattern of the product and all the diffraction peaks can be indexed to the cubic phase of Co_3O_4 (JCPDS 73-1701), indicating that Co_3O_4 products can also be obtained under these conditions.

As known, the properties of nanostructures depend greatly on the morphology and surface environments. Co_3O_4 has been extensively studied as an electrode material for lithium-ion batteries and supercapacitors.[7–11] In this paper, we studied the electrochemical properties of the obtained Co_3O_4 nanospheres by applying them as active materials for a supercapacitor electrode. The measurements were conducted using cyclic voltammetry (CV) in 1 M KOH electrolyte with a voltage window of 0–0.5 V and a scanning rate of 2–50 mV s^{-1}. The

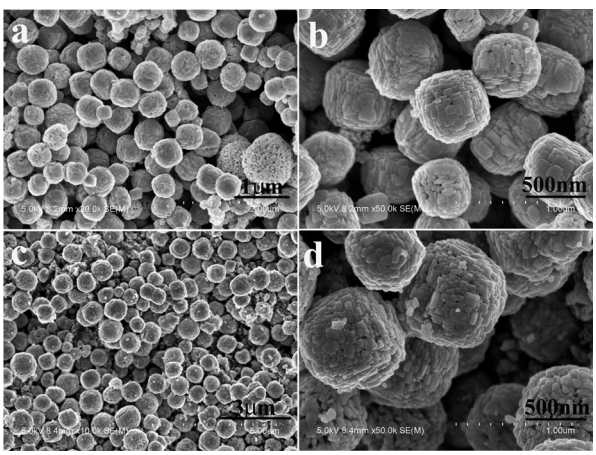

Fig. 5 SEM images of porous Co_3O_4 nanospheres prepared with different Cu^{2+} ions sources: (a, b) $CuCl_2$ and (c, d) $CuSO_4$.

Published on 11 May 2015. Downloaded on 9/25/2024 5:25:34 AM.

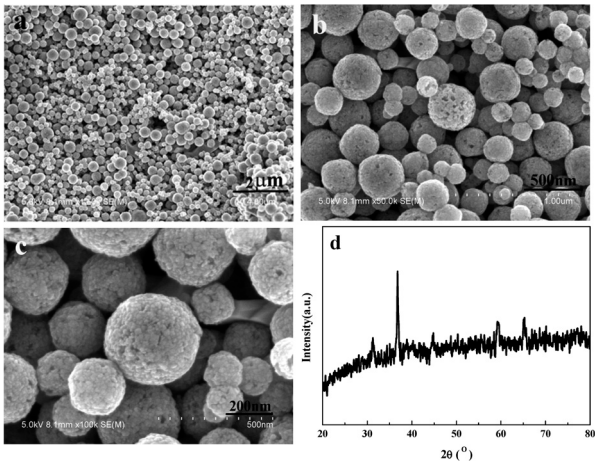

Fig. 6 (a–c) SEM images and (d) XRD pattern of the product prepared by adding $CoSO_4$ into $CuAc_2$ solution.

obtained CV curves are shown in Fig. 7. The CV curves are nearly symmetrical and display two pairs of redox peaks. The broad redox reaction peaks, which come from the redox processes of $Co_3O_4/CoOOH/CoO_2$, are characters of the electrochemical pseudocapacitors obtained from reversible faradaic redox reactions occurring within the electro-active materials.[20] As shown in Fig. 7a, when changing the scanning rate from 2–50 mV s^{-1}, the shape of the CV curves almost did not change, maybe because the electrode material is nano-sized, favors electron transfer and therefore lessens electrode polarization. Fig. 7b shows the CV curves of Co_3O_4 nanospheres and commercial Co_3O_4 at a scanning rate of 5 mV s^{-1}. The area under the CV curve of Co_3O_4 nanospheres is apparently much larger than that of commercial Co_3O_4, which indicates that Co_3O_4 nanospheres have a higher specific capacitance than commercial Co_3O_4. This is reasonable since the unique and nano structure of Co_3O_4 could provide fast ion and electron transfer and large reaction surface area, which are beneficial to the electrochemical performance.

Chronopotentiometry measurements confirm these results. Fig. 8a shows the charge–discharge curves of Co_3O_4 nanospheres and commercial Co_3O_4 powders obtained in the potential range of 0–0.45 V in 1 M KOH at a charge–discharge current of 0.5 A g^{-1}. The shapes of the charge–discharge curves show the characteristics of pseudo-capacitance, which are consistent with the results of the CV curves. Both samples present two variation ranges during the charge and discharge steps. The sloped curve at 0–0.45 V is characteristic of a typical pseudocapacitance, originating from electrochemical

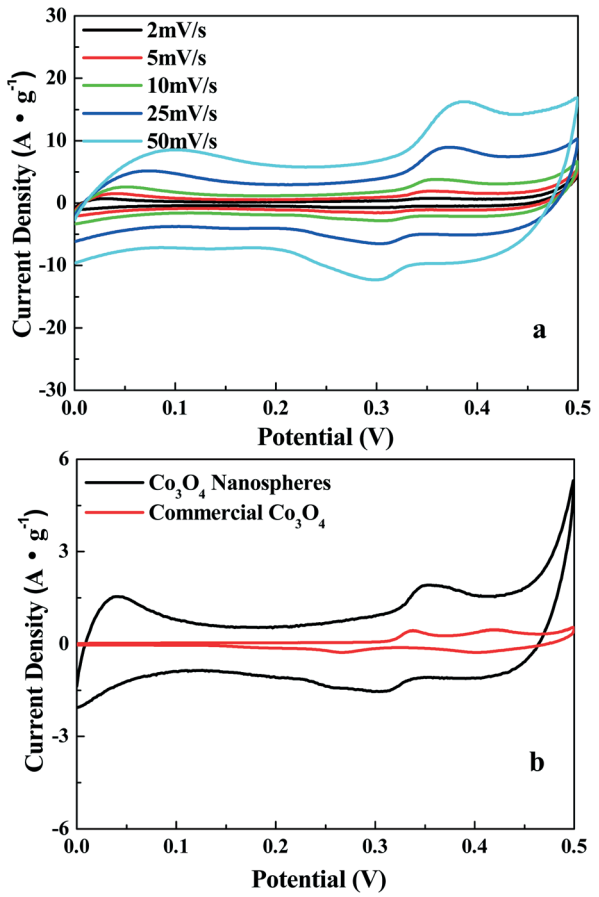

Fig. 7 (a) CV curves of porous Co_3O_4 nanospheres at a scanning rate of 2–50 mV s^{-1}; (b) CV curves of Co_3O_4 nanospheres and commercial Co_3O_4 at a scanning rate of 5 mV s^{-1}.

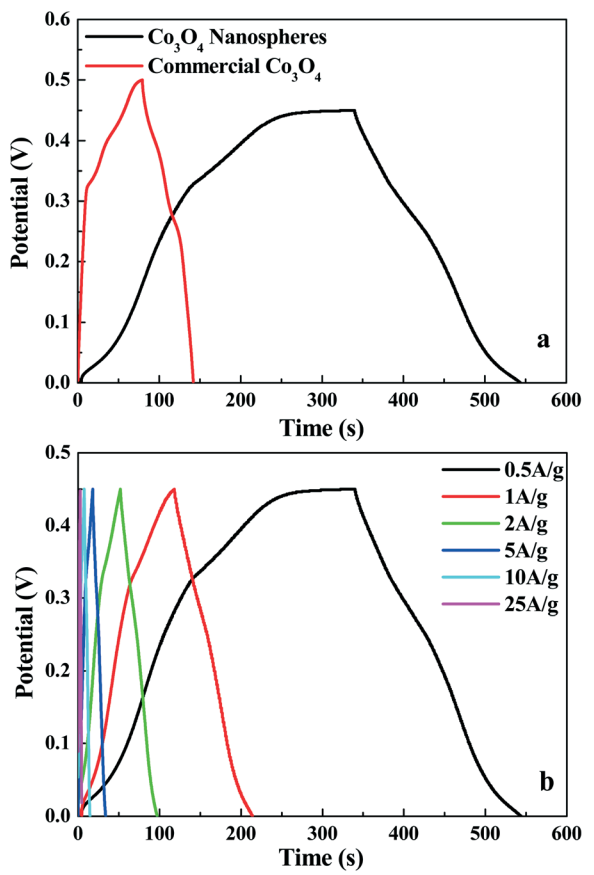

Fig. 8 Charge–discharge curves of (a) porous Co_3O_4 nanospheres and commercial Co_3O_4 powders at a charge–discharge current density of 0.5 A g^{-1}; (b) porous Co_3O_4 nanospheres at different current densities.

This journal is © The Royal Society of Chemistry 2015

Published on 11 May 2015. Downloaded on 9/25/2024 5:25:34 AM.

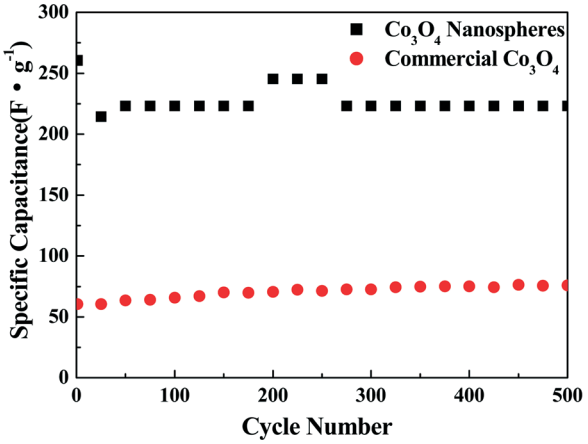

Fig. 9 Cycling properties of porous Co_3O_4 nanospheres and commercial Co_3O_4 powders at a current density of 1 A g^{-1}.

adsorption–desorption or a redox reaction at the electrode/electrolyte interface.[20] From the sloped curve at a discharge current of 0.5 A g^{-1}, the specific capacitances of Co_3O_4 nanospheres and commercial Co_3O_4 powders are calculated to be 246.7 F g^{-1} and 77 F g^{-1}, respectively. The specific capacitance of Co_3O_4 nanospheres is much larger than that of commercial Co_3O_4 powders, confirming the results from the CV curves. When the discharge current density is 0.5, 1, 2, 5, 10 and 25 A g^{-1}, the specific capacitance values of the Co_3O_4 nanospheres were calculated from the discharge curves in Fig. 8b to be 246.7 F g^{-1}, 213.3 F g^{-1}, 199 F g^{-1}, 174.4 F g^{-1}, 151.1 F g^{-1} and 105.6 F g^{-1}, respectively.

Since a long cycle life is a very important factor of supercapacitors, a cycle charge/discharge test has also been conducted to examine the service life of the Co_3O_4 nanospheres. Fig. 9 gives the variation of specific capacitance with cycle number at a current density of 1 A g^{-1} and reveals that the Co_3O_4 nanosphere electrode has good cycle properties as an excellent electrode material for electrochemical capacitors and the specific capacitance even grew a little larger in the first 500 cycles, which might be due to an electrochemical activation phenomenon.[27,28] Clearly, the Co_3O_4 nanosphere electrode shows better electrochemical capacitance performance than the commercial Co_3O_4 electrode. The high porosity structure of Co_3O_4 nanospheres minimizes both the ionic and electronic transportation distances in the cobalt oxide and thus improves the electrode kinetic performance, which is a crucial concern for high-power supercapacitor applications.

Conclusions

In summary, we successfully synthesized porous Co_3O_4 nanospheres by applying metal Cu^{2+} ions as structure-inducing agents. The porous Co_3O_4 nanospheres were composed of nanosheets. In the electrochemical measurement in a three-electrode system, the porous Co_3O_4 nanospheres exhibited a much better capacity of 246.7 F g^{-1} than commercial Co_3O_4 powder at a current density of 0.5 A g^{-1}, maintaining 86% of the initial capacity at a current density of 1 A g^{-1} after 500 cycles. Such high performance can be attributed to the desirable morphologies. The results manifest that porous Co_3O_4 nanospheres composed of nanosheets are promising electrode materials for supercapacitors in future application.

Acknowledgements

This work was supported by the National Natural Science Foundation of China (no. 21301002, 51302001 and 21441008), Anhui Province College Excellent Young Talents Fund (no. 2013SQRL037ZD and 2013SQRL036ZD) and Excellent Young Talents Support Plan of Anhui Province College.

Notes and references

1 M. Ando, T. Kobayashi, S. Iijima and M. Haruta, *J. Mater. Chem.*, 1997, **7**, 1779–1783.
2 A. M. Cao, J. S. Hu, H. P. Liang, W. G. Song, L. J. Wan, X. L. He, X. G. Gao and S. H. Xia, *J. Phys. Chem. B*, 2006, **110**, 15858–15863.
3 W. Y. Li, L. N. Xu and J. Chen, *Adv. Funct. Mater.*, 2005, **15**, 851–857.
4 S. Liu, Z. Y. Wang, H. R. Zhao, T. Fei and T. Zhang, *Sens. Actuators, B*, 2014, **197**, 342–349.
5 M. M. Natile and A. Glisenti, *Chem. Mater.*, 2002, **14**, 3090–3099.
6 L. H. Hu, Q. Peng and Y. D. Li, *J. Am. Chem. Soc.*, 2008, **130**, 16136–16137.
7 A. Q. Pan, Y. P. Wang, W. Xu, Z. W. Nie, S. Q. Liang, Z. M. Nie, C. M. Wang, G. Z. Cao and J. G. Zhang, *J. Power Sources*, 2014, **255**, 125–129.
8 X. W. Lou, D. Deng, J. Y. Lee, J. Feng and L. A. Areher, *Adv. Mater.*, 2008, **20**, 258–262.
9 H. T. Wang, L. Zhang, X. H. Tan, C. M. B. Holt, B. Zahiri, B. C. Olsen and D. Mitlin, *J. Phys. Chem. C*, 2011, **115**, 17599–17605.
10 Q. Yang, Z. Lu, X. Sun and J. Liu, *Sci. Rep.*, 2013, **3**, 3537.
11 W. Liu, L. Xu, D. Jiang, J. Qian, Q. Liu, X. W. Yang and K. Wang, *CrystEngComm*, 2014, **16**, 2395–2403.
12 A. S. Poyraz, W. A. Hines, C. H. Kuo, N. Li, D. M. Perry and S. L. Suib, *J. Appl. Phys.*, 2014, **115**, 114309.
13 J. P. Liu, J. Jiang, C. W. Cheng, H. X. Li, J. X. Zhang, H. Gong and H. J. Fan, *Adv. Mater.*, 2011, **23**, 2076–2081.
14 X. B. Zhao, Z. W. Pang, M. Z. Wu, X. S. Liu, H. Zhang, Y. Q. Ma, Z. Q. Sun, L. D. Zhang and X. S. Chen, *Mater. Res. Bull.*, 2013, **48**, 92–95.
15 R. Xu and H. C. Zeng, *J. Phys. Chem. B*, 2003, **107**, 12643–12649.
16 X. Y. Shi, S. B. Han, R. J. Sanedrin, C. Galvez, D. G. Ho, B. Hernandez, F. M. Zhou and M. Selke, *Nano Lett.*, 2002, **2**, 289–293.
17 S. Y. Xia, M. Q. Yu, J. Y. Hu, J. J. Feng, J. R. Chen, M. H. Shi and X. X. Weng, *Electrochem. Commun.*, 2014, **40**, 67–70.
18 H. S. Jadhav, A. K. Rai, J. Y. Lee, J. Kim and C. J. Park, *Electrochim. Acta*, 2014, **146**, 270–277.

19 Y. H. Xiao, S. J. Liu, F. Li, A. Q. Zhang, J. H. Zhao, S. M. Fang and D. Z. Jia, *Adv. Funct. Mater.*, 2012, **22**, 4052–4059.
20 W. Du, R. M. Liu, Y. W. Jiang, Q. Y. Lu, Y. Z. Fan and F. Gao, *J. Power Sources*, 2013, **227**, 101–105.
21 Y. Z. Zhang, Y. Wang, Y. L. Xie, T. Cheng, W. Y. Lai, H. Pang and W. Huang, *Nanoscale*, 2014, **6**, 14354–14359.
22 M. Büyükyazi, C. Hegemann, T. Lehnen, W. Tyrra and S. Mathur, *Inorg. Chem.*, 2014, **53**, 10928–10936.
23 H. W. Che, A. F. Liu, J. X. Hou, J. B. Mu, Y. M. Bai, S. F. Zhao, X. L. Zhang and H. J. He, *J. Mater. Sci.: Mater. Electron.*, 2014, **25**, 3209–3218.
24 R. Xu, J. W. Wang, Q. Y. Li, G. Y. Sun, E. B. Wang, S. H. Li, J. M. Gu and M. L. Ju, *J. Solid State Chem.*, 2009, **182**, 3177–3182.
25 H. Pang, S. M. Wang, G. C. Li, Y. H. Ma, J. Li, X. X. Li, L. Zhang, J. S. Zhang and H. H. Zheng, *J. Mater. Chem. A*, 2013, **1**, 5053–5060.
26 R. M. Liu, Y. W. Jiang, H. Fan, Q. Y. Lu, W. Du and F. Gao, *Chem. – Eur. J.*, 2012, **18**, 8957–8963.
27 C. C. Hu, K. H. Chang and T. Y. Hsu, *J. Electrochem. Soc.*, 2008, **155**, F196–F200.
28 H. B. Wu, H. Pang and X. W. Lou, *Energy Environ. Sci.*, 2013, **6**, 3619–3626.

Published on 11 May 2015. Downloaded on 9/25/2024 5:25:34 AM.

This journal is © The Royal Society of Chemistry 2015